

First Measurement of the Decay Asymmetry in the pure W -boson-exchange Decay $\Lambda_c^+ \rightarrow \Xi^0 K^+$

M. Ablikim,¹ M. N. Achasov,^{5,b} P. Adlarson,⁷⁴ X. C. Ai,⁸⁰ R. Aliberti,³⁵ A. Amoroso,^{73a,73c} M. R. An,³⁹ Q. An,^{70,57} Y. Bai,⁵⁶ O. Bakina,³⁶ I. Balossino,^{29a} Y. Ban,^{46,g} V. Batozskaya,^{1,44} K. Begzsuren,³² N. Berger,³⁵ M. Berlowski,⁴⁴ M. Bertani,^{28a} D. Bettoni,^{29a} F. Bianchi,^{73a,73c} E. Bianco,^{73a,73c} A. Bortone,^{73a,73c} I. Boyko,³⁶ R. A. Briere,⁶ A. Brueggemann,⁶⁷ H. Cai,⁷⁵ X. Cai,^{1,57} A. Calcaterra,^{28a} G. F. Cao,^{1,62} N. Cao,^{1,62} S. A. Cetin,^{61a} J. F. Chang,^{1,57} T. T. Chang,⁷⁶ W. L. Chang,^{1,62} G. R. Che,⁴³ G. Chelkov,^{36,a} C. Chen,⁴³ Chao Chen,⁵⁴ G. Chen,¹ H. S. Chen,^{1,62} M. L. Chen,^{1,57,62} S. J. Chen,⁴² S. M. Chen,⁶⁰ T. Chen,^{1,62} X. R. Chen,^{31,62} X. T. Chen,^{1,62} Y. B. Chen,^{1,57} Y. Q. Chen,³⁴ Z. J. Chen,^{25,h} W. S. Cheng,^{73c} S. K. Choi,¹¹ X. Chu,⁴³ G. Cibinetto,^{29a} S. C. Coen,⁴ F. Cossio,^{73c} J. J. Cui,⁴⁹ H. L. Dai,^{1,57} J. P. Dai,⁷⁸ A. Dbeysi,¹⁸ R. E. de Boer,⁴ D. Dedovich,³⁶ Z. Y. Deng,¹ A. Denig,³⁵ I. Denysenko,³⁶ M. Destefanis,^{73a,73c} F. De Mori,^{73a,73c} B. Ding,^{65,1} X. X. Ding,^{46,g} Y. Ding,⁴⁰ Y. Ding,³⁴ J. Dong,^{1,57} L. Y. Dong,^{1,62} M. Y. Dong,^{1,57,62} X. Dong,⁷⁵ M. C. Du,¹ S. X. Du,⁸⁰ Z. H. Duan,⁴² P. Egorov,^{36,a} Y. H. Y. Fan,⁴⁵ Y. L. Fan,⁷⁵ J. Fang,^{1,57} S. S. Fang,^{1,62} W. X. Fang,¹ Y. Fang,¹ R. Farinelli,^{29a} L. Fava,^{73b,73c} F. Feldbauer,⁴ G. Felici,^{28a} C. Q. Feng,^{70,57} J. H. Feng,⁵⁸ K. Fischer,⁶⁸ M. Fritsch,⁴ C. Fritsch,⁶⁷ C. D. Fu,¹ J. L. Fu,⁶² Y. W. Fu,¹ H. Gao,⁶² Y. N. Gao,^{46,g} Yang Gao,^{70,57} S. Garbolino,^{73c} I. Garzia,^{29a,29b} P. T. Ge,⁷⁵ Z. W. Ge,⁴² C. Geng,⁵⁸ E. M. Gersabeck,⁶⁶ A. Gilman,⁶⁸ K. Goetzen,¹⁴ L. Gong,⁴⁰ W. X. Gong,^{1,57} W. Gradl,³⁵ S. Gramigna,^{29a,29b} M. Greco,^{73a,73c} M. H. Gu,^{1,57} C. Y. Guan,^{31,62} Z. L. Guan,²² A. Q. Guo,^{31,62} L. B. Guo,⁴¹ M. J. Guo,⁴⁹ R. P. Guo,⁴⁸ Y. P. Guo,^{13,f} A. Guskov,^{36,a} T. T. Han,⁴⁹ W. Y. Han,³⁹ X. Q. Hao,¹⁹ F. A. Harris,⁶⁴ K. K. He,⁵⁴ K. L. He,^{1,62} F. H. H. Heinsius,⁴ C. H. Heinz,³⁵ Y. K. Heng,^{1,57,62} C. Herold,⁵⁹ T. Holtmann,⁴ P. C. Hong,^{13,f} G. Y. Hou,^{1,62} X. T. Hou,^{1,62} Y. R. Hou,⁶² Z. L. Hou,¹ H. M. Hu,^{1,62} J. F. Hu,^{55,i} T. Hu,^{1,57,62} Y. Hu,¹ G. S. Huang,^{70,57} K. X. Huang,⁵⁸ L. Q. Huang,^{31,62} X. T. Huang,⁴⁹ Y. P. Huang,¹ T. Hussain,⁷² N. Hüsken,^{27,35} W. Imoehl,²⁷ J. Jackson,²⁷ S. Jaeger,⁴ S. Janchiv,³² J. H. Jeong,¹¹ Q. Ji,¹ Q. P. Ji,¹⁹ X. B. Ji,^{1,62} X. L. Ji,^{1,57} Y. Y. Ji,⁴⁹ X. Q. Jia,⁴⁹ Z. K. Jia,^{70,57} H. J. Jiang,⁷⁵ P. C. Jiang,^{46,g} S. S. Jiang,³⁹ T. J. Jiang,¹⁶ X. S. Jiang,^{1,57,62} Y. Jiang,⁶² J. B. Jiao,⁴⁹ Z. Jiao,²³ S. Jin,⁴² Y. Jin,⁶⁵ M. Q. Jing,^{1,62} T. Johansson,⁷⁴ X. K.,¹ S. Kabana,³³ N. Kalantar-Nayestanaki,⁶³ X. L. Kang,¹⁰ X. S. Kang,⁴⁰ R. Kappert,⁶³ M. Kavatsyuk,⁶³ B. C. Ke,⁸⁰ A. Khoukaz,⁶⁷ R. Kiuchi,¹ R. Kliemt,¹⁴ O. B. Kolcu,^{61a} B. Kopf,⁴ M. Kuessner,⁴ A. Kupsc,^{44,74} W. Kühn,³⁷ J. J. Lane,⁶⁶ P. Larin,¹⁸ A. Lavania,²⁶ L. Lavezzi,^{73a,73c} T. T. Lei,^{70,k} Z. H. Lei,^{70,57} H. Leithoff,³⁵ M. Lellmann,³⁵ T. Lenz,³⁵ C. Li,⁴⁷ C. Li,⁴³ C. H. Li,³⁹ Cheng Li,^{70,57} D. M. Li,⁸⁰ F. Li,^{1,57} G. Li,¹ H. Li,^{70,57} H. B. Li,^{1,62} H. J. Li,¹⁹ H. N. Li,^{55,i} Hui Li,⁴³ J. R. Li,⁶⁰ J. S. Li,⁵⁸ J. W. Li,⁴⁹ K. L. Li,¹⁹ Ke Li,¹ L. J. Li,^{1,62} L. K. Li,¹ Lei Li,³ M. H. Li,⁴³ P. R. Li,^{38,j,k} Q. X. Li,⁴⁹ S. X. Li,¹³ T. Li,⁴⁹ W. D. Li,^{1,62} W. G. Li,¹ X. H. Li,^{70,57} X. L. Li,⁴⁹ Xiaoyu Li,^{1,62} Y. G. Li,^{46,g} Z. J. Li,⁵⁸ C. Liang,⁴² H. Liang,^{1,62} H. Liang,^{70,57} H. Liang,³⁴ Y. F. Liang,⁵³ Y. T. Liang,^{31,62} G. R. Liao,¹⁵ L. Z. Liao,⁴⁹ Y. P. Liao,^{1,62} J. Libby,²⁶ A. Limphirat,⁵⁹ D. X. Lin,^{31,62} T. Lin,¹ B. J. Liu,¹ B. X. Liu,⁷⁵ C. Liu,³⁴ C. X. Liu,¹ F. H. Liu,⁵² Fang Liu,¹ Feng Liu,⁷ G. M. Liu,^{55,i} H. Liu,^{38,j,k} H. M. Liu,^{1,62} Huanhuan Liu,¹ Huihui Liu,²¹ J. B. Liu,^{70,57} J. L. Liu,⁷¹ J. Y. Liu,^{1,62} K. Liu,¹ K. Y. Liu,⁴⁰ Ke Liu,²² L. Liu,^{70,57} L. C. Liu,⁴³ Lu Liu,⁴³ M. H. Liu,^{13,f} P. L. Liu,¹ Q. Liu,⁶² S. B. Liu,^{70,57} T. Liu,^{13,f} W. K. Liu,⁴³ W. M. Liu,^{70,57} X. Liu,^{38,j,k} Y. Liu,^{38,j,k} Y. Liu,⁸⁰ Y. B. Liu,⁴³ Z. A. Liu,^{1,57,62} Z. Q. Liu,⁴⁹ X. C. Lou,^{1,57,62} F. X. Lu,⁵⁸ H. J. Lu,²³ J. G. Lu,^{1,57} X. L. Lu,¹ Y. Lu,⁸ Y. P. Lu,^{1,57} Z. H. Lu,^{1,62} C. L. Luo,⁴¹ M. X. Luo,⁷⁹ T. Luo,^{13,f} X. L. Luo,^{1,57} X. R. Lyu,⁶² Y. F. Lyu,⁴³ F. C. Ma,⁴⁰ H. L. Ma,¹ J. L. Ma,^{1,62} L. L. Ma,⁴⁹ M. M. Ma,^{1,62} Q. M. Ma,¹ R. Q. Ma,^{1,62} R. T. Ma,⁶² X. Y. Ma,^{1,57} Y. Ma,^{46,g} Y. M. Ma,³¹ F. E. Maas,¹⁸ M. Maggiora,^{73a,73c} S. Malde,⁶⁸ Q. A. Malik,⁷² A. Mangoni,^{28b} Y. J. Mao,^{46,g} Z. P. Mao,¹ S. Marcello,^{73a,73c} Z. X. Meng,⁶⁵ J. G. Messchendorp,^{14,63} G. Mezzadri,^{29a} H. Miao,^{1,62} T. J. Min,⁴² R. E. Mitchell,²⁷ X. H. Mo,^{1,57,62} N. Yu. Muchnoi,^{5,b} J. Muskalla,³⁵ Y. Nefedov,³⁶ F. Nerling,^{18,d} I. B. Nikolaev,^{5,b} Z. Ning,^{1,57} S. Nisar,^{12,l} Y. Niu,⁴⁹ S. L. Olsen,⁶² Q. Ouyang,^{1,57,62} S. Pacetti,^{28b,28c} X. Pan,⁵⁴ Y. Pan,⁵⁶ A. Pathak,³⁴ P. Patteri,^{28a} Y. P. Pei,^{70,57} M. Pelizzaeus,⁴ H. P. Peng,^{70,57} K. Peters,^{14,d} J. L. Ping,⁴¹ R. G. Ping,^{1,62} S. Plura,³⁵ S. Pogodin,³⁶ V. Prasad,³³ F. Z. Qi,¹ H. Qi,^{70,57} H. R. Qi,⁶⁰ M. Qi,⁴² T. Y. Qi,^{13,f} S. Qian,^{1,57} W. B. Qian,⁶² C. F. Qiao,⁶² J. J. Qin,⁷¹ L. Q. Qin,¹⁵ X. P. Qin,^{13,f} X. S. Qin,⁴⁹ Z. H. Qin,^{1,57} J. F. Qiu,¹ S. Q. Qu,⁶⁰ C. F. Redmer,³⁵ K. J. Ren,³⁹ A. Rivetti,^{73c} V. Rodin,⁶³ M. Rolo,^{73c} G. Rong,^{1,62} Ch. Rosner,¹⁸ S. N. Ruan,⁴³ N. Salone,⁴⁴ A. Sarantsev,^{36,c} Y. Schelhaas,³⁵ K. Schoenning,⁷⁴ M. Scodreggio,^{29a,29b} K. Y. Shan,^{13,f} W. Shan,²⁴ X. Y. Shan,^{70,57} J. F. Shangguan,⁵⁴ L. G. Shao,^{1,62} M. Shao,^{70,57} C. P. Shen,^{13,f} H. F. Shen,^{1,62} W. H. Shen,⁶² X. Y. Shen,^{1,62} B. A. Shi,⁶² H. C. Shi,^{70,57} J. L. Shi,¹³ J. Y. Shi,¹ Q. Q. Shi,⁵⁴ R. S. Shi,^{1,62} X. Shi,^{1,57} J. J. Song,¹⁹ T. Z. Song,⁵⁸ W. M. Song,^{34,1} Y. J. Song,¹³ Y. X. Song,^{46,g} S. Sosio,^{73a,73c} S. Spataro,^{73a,73c} F. Stieler,³⁵ Y. J. Su,⁶² G. B. Sun,⁷⁵ G. X. Sun,¹ H. Sun,⁶² H. K. Sun,¹ J. F. Sun,¹⁹ K. Sun,⁶⁰ L. Sun,⁷⁵ S. S. Sun,^{1,62} T. Sun,^{1,62} W. Y. Sun,³⁴ Y. Sun,¹⁰ Y. J. Sun,^{70,57} Y. Z. Sun,¹ Z. T. Sun,⁴⁹ Y. X. Tan,^{70,57} C. J. Tang,⁵³ G. Y. Tang,¹ J. Tang,⁵⁸ Y. A. Tang,⁷⁵ L. Y. Tao,⁷¹ Q. T. Tao,^{25,h} M. Tat,⁶⁸ J. X. Teng,^{70,57} V. Thoren,⁷⁴ W. H. Tian,⁵⁸ W. H. Tian,⁵¹ Y. Tian,^{31,62} Z. F. Tian,⁷⁵ I. Uman,^{61b} S. J. Wang,⁴⁹ B. Wang,¹ B. L. Wang,⁶² Bo Wang,^{70,57} C. W. Wang,⁴² D. Y. Wang,^{46,g} F. Wang,⁷¹ H. J. Wang,^{38,j,k} H. P. Wang,^{1,62} J. P. Wang,⁴⁹ K. Wang,^{1,57} L. L. Wang,¹ M. Wang,⁴⁹ Meng Wang,^{1,62} S. Wang,^{13,f} S. Wang,^{38,j,k} T. Wang,^{13,f} T. J. Wang,⁴³ W. Wang,⁵⁸ W. Wang,⁷¹ W. P. Wang,^{70,57} X. Wang,^{46,g} X. F. Wang,^{38,j,k} X. J. Wang,³⁹ X. L. Wang,^{13,f} Y. Wang,⁶⁰ Y. D. Wang,⁴⁵ Y. F. Wang,^{1,57,62} Y. H. Wang,⁴⁷ Y. N. Wang,⁴⁵ Y. Q. Wang,¹ Yaqian Wang,^{17,1} Yi Wang,⁶⁰ Z. Wang,^{1,57} Z. L. Wang,⁷¹ Z. Y. Wang,^{1,62} Ziyi Wang,⁶² D. Wei,⁶⁹ D. H. Wei,¹⁵ F. Wiedner,⁶⁷ S. P. Wen,¹ C. W. Wenzel,⁴ U. Wiedner,⁴ G. Wilkinson,⁶⁸ M. Wolke,⁷⁴ L. Wollenberg,⁴ C. Wu,³⁹ J. F. Wu,^{1,62} L. H. Wu,¹ L. J. Wu,^{1,62} X. Wu,^{13,f} X. H. Wu,³⁴ Y. Wu,⁷⁰ Y. J. Wu,³¹ Z. Wu,^{1,57} L. Xia,^{70,57} X. M. Xian,³⁹ T. Xiang,^{46,g} D. Xiao,^{38,j,k} G. Y. Xiao,⁴² S. Y. Xiao,¹ Y. L. Xiao,^{13,f} Z. J. Xiao,⁴¹ C. Xie,⁴² X. H. Xie,^{46,g} Y. Xie,⁴⁹ Y. G. Xie,^{1,57} Y. H. Xie,⁷ Z. P. Xie,^{70,57} T. Y. Xing,^{1,62} C. F. Xu,^{1,62} C. J. Xu,⁵⁸ G. F. Xu,¹ H. Y. Xu,⁶⁵ Q. J. Xu,¹⁶ Q. N. Xu,³⁰ W. Xu,^{1,62} W. L. Xu,⁶⁵ X. P. Xu,⁵⁴ Y. C. Xu,⁷⁷ Z. P. Xu,⁴² Z. S. Xu,⁶² F. Yan,^{13,f} L. Yan,^{13,f} W. B. Yan,^{70,57} W. C. Yan,⁸⁰ X. Q. Yan,¹ H. J. Yang,^{50,e} H. L. Yang,³⁴ H. X. Yang,¹ Tao Yang,¹ Y. Yang,^{13,f} Y. F. Yang,⁴³ Y. X. Yang,^{1,62} Yifan Yang,^{1,62}

Z. W. Yang,^{38,j,k} Z. P. Yao,⁴⁹ M. Ye,^{1,57} M. H. Ye,⁹ J. H. Yin,¹ Z. Y. You,⁵⁸ B. X. Yu,^{1,57,62} C. X. Yu,⁴³ G. Yu,^{1,62}
 J. S. Yu,^{25,h} T. Yu,⁷¹ X. D. Yu,^{46,g} C. Z. Yuan,^{1,62} L. Yuan,² S. C. Yuan,¹ X. Q. Yuan,¹ Y. Yuan,^{1,62} Z. Y. Yuan,⁵⁸
 C. X. Yue,³⁹ A. A. Zafar,⁷² F. R. Zeng,⁴⁹ X. Zeng,^{13,f} Y. Zeng,^{25,h} Y. J. Zeng,^{1,62} X. Y. Zhai,³⁴ Y. C. Zhai,⁴⁹ Y. H. Zhan,⁵⁸
 A. Q. Zhang,^{1,62} B. L. Zhang,^{1,62} B. X. Zhang,¹ D. H. Zhang,⁴³ G. Y. Zhang,¹⁹ H. Zhang,⁷⁰ H. H. Zhang,⁵⁸ H. H. Zhang,³⁴
 H. Q. Zhang,^{1,57,62} H. Y. Zhang,^{1,57} J. Zhang,⁸⁰ J. J. Zhang,⁵¹ J. L. Zhang,²⁰ J. Q. Zhang,⁴¹ J. W. Zhang,^{1,57,62}
 J. X. Zhang,^{38,j,k} J. Y. Zhang,¹ J. Z. Zhang,^{1,62} Jianyu Zhang,⁶² Jiawei Zhang,^{1,62} L. M. Zhang,⁶⁰ L. Q. Zhang,⁵⁸
 Lei Zhang,⁴² P. Zhang,^{1,62} Q. Y. Zhang,^{39,80} Shuihan Zhang,^{1,62} Shulei Zhang,^{25,h} X. D. Zhang,⁴⁵ X. M. Zhang,¹
 X. Y. Zhang,⁴⁹ Xuyan Zhang,⁵⁴ Y. Zhang,⁷¹ Y. Zhang,⁶⁸ Y. T. Zhang,⁸⁰ Y. H. Zhang,^{1,57} Yan Zhang,^{70,57} Yao Zhang,¹
 Z. H. Zhang,¹ Z. L. Zhang,³⁴ Z. Y. Zhang,⁷⁵ Z. Y. Zhang,⁴³ G. Zhao,¹ J. Zhao,³⁹ J. Y. Zhao,^{1,62} J. Z. Zhao,^{1,57} Lei Zhao,^{70,57}
 Ling Zhao,¹ M. G. Zhao,⁴³ S. J. Zhao,⁸⁰ Y. B. Zhao,^{1,57} Y. X. Zhao,^{31,62} Z. G. Zhao,^{70,57} A. Zhemchugov,^{36,a} B. Zheng,⁷¹
 J. P. Zheng,^{1,57} W. J. Zheng,^{1,62} Y. H. Zheng,⁶² B. Zhong,⁴¹ X. Zhong,⁵⁸ H. Zhou,⁴⁹ L. P. Zhou,^{1,62} X. Zhou,⁷⁵ X. K. Zhou,⁷
 X. R. Zhou,^{70,57} X. Y. Zhou,³⁹ Y. Z. Zhou,^{13,f} J. Zhu,⁴³ K. Zhu,¹ K. J. Zhu,^{1,57,62} L. Zhu,³⁴ L. X. Zhu,⁶² S. H. Zhu,⁶⁹
 S. Q. Zhu,⁴² T. J. Zhu,^{13,f} W. J. Zhu,^{13,f} Y. C. Zhu,^{70,57} Z. A. Zhu,^{1,62} J. H. Zou,¹ J. Zu,^{70,57},

(BESIII Collaboration)

¹ Institute of High Energy Physics, Beijing 100049, People's Republic of China

² Beihang University, Beijing 100191, People's Republic of China

³ Beijing Institute of Petrochemical Technology, Beijing 102617, People's Republic of China

⁴ Bochum Ruhr-University, D-44780 Bochum, Germany

⁵ Budker Institute of Nuclear Physics SB RAS (BINP), Novosibirsk 630090, Russia

⁶ Carnegie Mellon University, Pittsburgh, Pennsylvania 15213, USA

⁷ Central China Normal University, Wuhan 430079, People's Republic of China

⁸ Central South University, Changsha 410083, People's Republic of China

⁹ China Center of Advanced Science and Technology, Beijing 100190, People's Republic of China

¹⁰ China University of Geosciences, Wuhan 430074, People's Republic of China

¹¹ Chung-Ang University, Seoul, 06974, Republic of Korea

¹² COMSATS University Islamabad, Lahore Campus, Defence Road, Off Raiwind Road, 54000 Lahore, Pakistan

¹³ Fudan University, Shanghai 200433, People's Republic of China

¹⁴ GSI Helmholtzcentre for Heavy Ion Research GmbH, D-64291 Darmstadt, Germany

¹⁵ Guangxi Normal University, Guilin 541004, People's Republic of China

¹⁶ Hangzhou Normal University, Hangzhou 310036, People's Republic of China

¹⁷ Hebei University, Baoding 071002, People's Republic of China

¹⁸ Helmholtz Institute Mainz, Staudinger Weg 18, D-55099 Mainz, Germany

¹⁹ Henan Normal University, Xinxiang 453007, People's Republic of China

²⁰ Henan University, Kaifeng 475004, People's Republic of China

²¹ Henan University of Science and Technology, Luoyang 471003, People's Republic of China

²² Henan University of Technology, Zhengzhou 450001, People's Republic of China

²³ Huangshan College, Huangshan 245000, People's Republic of China

²⁴ Hunan Normal University, Changsha 410081, People's Republic of China

²⁵ Hunan University, Changsha 410082, People's Republic of China

²⁶ Indian Institute of Technology Madras, Chennai 600036, India

²⁷ Indiana University, Bloomington, Indiana 47405, USA

^{28a} INFN Laboratori Nazionali di Frascati, INFN Laboratori Nazionali di Frascati, I-00044, Frascati, Italy

^{28b} INFN Sezione di Perugia, I-06100, Perugia, Italy

^{28c} University of Perugia, I-06100, Perugia, Italy

^{29a} INFN Sezione di Ferrara, INFN Sezione di Ferrara, I-44122, Ferrara, Italy

^{29b} University of Ferrara, I-44122, Ferrara, Italy

³⁰ Inner Mongolia University, Hohhot 010021, People's Republic of China

³¹ Institute of Modern Physics, Lanzhou 730000, People's Republic of China

³² Institute of Physics and Technology, Peace Avenue 54B, Ulaanbaatar 13330, Mongolia

³³ Instituto de Alta Investigación, Universidad de Tarapacá, Casilla 7D, Arica 1000000, Chile

³⁴ Jilin University, Changchun 130012, People's Republic of China

³⁵ Johannes Gutenberg University of Mainz, Johann-Joachim-Becher-Weg 45, D-55099 Mainz, Germany

³⁶ Joint Institute for Nuclear Research, 141980 Dubna, Moscow region, Russia

³⁷ Justus-Liebig-Universität Giessen, II. Physikalisches Institut, Heinrich-Buff-Ring 16, D-35392 Giessen, Germany

³⁸ Lanzhou University, Lanzhou 730000, People's Republic of China

³⁹ Liaoning Normal University, Dalian 116029, People's Republic of China

⁴⁰ Liaoning University, Shenyang 110036, People's Republic of China

⁴¹ Nanjing Normal University, Nanjing 210023, People's Republic of China

⁴² Nanjing University, Nanjing 210093, People's Republic of China

⁴³ Nankai University, Tianjin 300071, People's Republic of China

⁴⁴ National Centre for Nuclear Research, Warsaw 02-093, Poland

⁴⁵ North China Electric Power University, Beijing 102206, People's Republic of China

- ⁴⁶ Peking University, Beijing 100871, People's Republic of China
- ⁴⁷ Qufu Normal University, Qufu 273165, People's Republic of China
- ⁴⁸ Shandong Normal University, Jinan 250014, People's Republic of China
- ⁴⁹ Shandong University, Jinan 250100, People's Republic of China
- ⁵⁰ Shanghai Jiao Tong University, Shanghai 200240, People's Republic of China
- ⁵¹ Shanxi Normal University, Linfen 041004, People's Republic of China
- ⁵² Shanxi University, Taiyuan 030006, People's Republic of China
- ⁵³ Sichuan University, Chengdu 610064, People's Republic of China
- ⁵⁴ Soochow University, Suzhou 215006, People's Republic of China
- ⁵⁵ South China Normal University, Guangzhou 510006, People's Republic of China
- ⁵⁶ Southeast University, Nanjing 211100, People's Republic of China
- ⁵⁷ State Key Laboratory of Particle Detection and Electronics, Beijing 100049, Hefei 230026, People's Republic of China
- ⁵⁸ Sun Yat-Sen University, Guangzhou 510275, People's Republic of China
- ⁵⁹ Suranaree University of Technology, University Avenue 111, Nakhon Ratchasima 30000, Thailand
- ⁶⁰ Tsinghua University, Beijing 100084, People's Republic of China
- ^{61a} Turkish Accelerator Center Particle Factory Group, Istinye University, 34010, Istanbul, Turkey
- ^{61b} Near East University, Nicosia, North Cyprus, 99138, Mersin 10, Turkey
- ⁶² University of Chinese Academy of Sciences, Beijing 100049, People's Republic of China
- ⁶³ University of Groningen, NL-9747 AA Groningen, The Netherlands
- ⁶⁴ University of Hawaii, Honolulu, Hawaii 96822, USA
- ⁶⁵ University of Jinan, Jinan 250022, People's Republic of China
- ⁶⁶ University of Manchester, Oxford Road, Manchester, M13 9PL, United Kingdom
- ⁶⁷ University of Muenster, Wilhelm-Klemm-Strasse 9, 48149 Muenster, Germany
- ⁶⁸ University of Oxford, Keble Road, Oxford OX13RH, United Kingdom
- ⁶⁹ University of Science and Technology Liaoning, Anshan 114051, People's Republic of China
- ⁷⁰ University of Science and Technology of China, Hefei 230026, People's Republic of China
- ⁷¹ University of South China, Hengyang 421001, People's Republic of China
- ⁷² University of the Punjab, Lahore-54590, Pakistan
- ^{73a} University of Turin and INFN, University of Turin, I-10125, Turin, Italy
- ^{73b} University of Eastern Piedmont, I-15121, Alessandria, Italy
- ^{73c} INFN, I-10125, Turin, Italy
- ⁷⁴ Uppsala University, Box 516, SE-75120 Uppsala, Sweden
- ⁷⁵ Wuhan University, Wuhan 430072, People's Republic of China
- ⁷⁶ Xinyang Normal University, Xinyang 464000, People's Republic of China
- ⁷⁷ Yantai University, Yantai 264005, People's Republic of China
- ⁷⁸ Yunnan University, Kunming 650500, People's Republic of China
- ⁷⁹ Zhejiang University, Hangzhou 310027, People's Republic of China
- ⁸⁰ Zhengzhou University, Zhengzhou 450001, People's Republic of China
- ^a Also at the Moscow Institute of Physics and Technology, Moscow 141700, Russia
- ^b Also at the Novosibirsk State University, Novosibirsk, 630090, Russia
- ^c Also at the NRC "Kurchatov Institute", PNPI, 188300, Gatchina, Russia
- ^d Also at Goethe University Frankfurt, 60323 Frankfurt am Main, Germany
- ^e Also at Key Laboratory for Particle Physics, Astrophysics and Cosmology, Ministry of Education; Shanghai Key Laboratory for Particle Physics and Cosmology; Institute of Nuclear and Particle Physics, Shanghai 200240, People's Republic of China
- ^f Also at Key Laboratory of Nuclear Physics and Ion-beam Application (MOE) and Institute of Modern Physics, Fudan University, Shanghai 200443, People's Republic of China
- ^g Also at State Key Laboratory of Nuclear Physics and Technology, Peking University, Beijing 100871, People's Republic of China
- ^h Also at School of Physics and Electronics, Hunan University, Changsha 410082, China
- ⁱ Also at Guangdong Provincial Key Laboratory of Nuclear Science, Institute of Quantum Matter, South China Normal University, Guangzhou 510006, China
- ^j Also at MOE Frontiers Science Center for Rare Isotopes, Lanzhou University, Lanzhou 730000, People's Republic of China
- ^k Also at Lanzhou Center for Theoretical Physics, Lanzhou University, Lanzhou 730000, People's Republic of China
- ^l Also at the Department of Mathematical Sciences, IBA, Karachi 75270, Pakistan

(Dated: **January 23, 2024**)

Based on 4.4 fb^{-1} of e^+e^- annihilation data collected at the center-of-mass energies between 4.60 and 4.70 GeV with the BESIII detector at the BEPCII collider, the pure W -boson-exchange decay $\Lambda_c^+ \rightarrow \Xi^0 K^+$ is studied with a full angular analysis. The corresponding decay asymmetry is measured for the first time to be $\alpha_{\Xi^0 K^+} = 0.01 \pm 0.16(\text{stat.}) \pm 0.03(\text{syst.})$. This result reflects the non-interference effect between the S - and P -wave amplitudes. The phase shift between S - and P -wave amplitudes has two solutions, which are $\delta_p - \delta_s = -1.55 \pm 0.25(\text{stat.}) \pm 0.05(\text{syst.}) \text{ rad}$ or $1.59 \pm 0.25(\text{stat.}) \pm 0.05(\text{syst.}) \text{ rad}$.

Investigations of charmed baryon decay dynamics are essential to explore the weak and strong interactions in the Standard Model (SM) of particle physics. The ground state of the singly-charmed baryons Λ_c^+ was discovered in 1979 [1]. Many studies have since been made of the properties of charmed baryons, such as the decay branching fractions (BFs) and decay asymmetries. But experimental results of the decay asymmetries, which are sensitive to the different amplitudes in the decay dynamics, were only a few. Since 2014, there has been some progress on the weak hadronic decays of Λ_c^+ , $\Xi_c^{+,0}$, and Ω_c^0 , both experimentally and theoretically [2–4]. This provides crucial information about the properties of all the singly-charmed baryons and the searches for doubly-charmed baryons (Ξ_{cc} and Ω_{cc}) [5]. Nonetheless, the understanding of the decay dynamics of charmed baryons is still limited, due to the lack of precision experimental measurements and the difficulties in the theoretical treatment of strong interaction effects.

Compared to heavy meson decays, charmed baryon decays have a significant dependence on nonfactorizable contributions from W -boson-exchange diagrams. However, these contributions cannot currently be calculated using theoretical approaches. Additionally, no experimental measurements exist for the decay asymmetries of W -boson-exchange hadronic decays. An example of such a process is the decay $\Lambda_c^+ \rightarrow \Xi^0 K^+$, which can only be produced via a W -boson-exchange process as depicted in Fig. 1. Experimental measurements of the asymmetry parameters of the decay $\Lambda_c^+ \rightarrow \Xi^0 K^+$ can aid understanding of the internal dynamics and can also explore charge-parity (CP) violation in baryons [6].

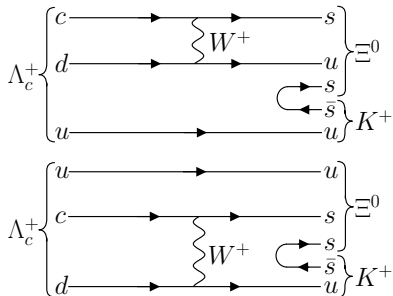


FIG. 1. Feynman diagrams for $\Lambda_c^+ \rightarrow \Xi^0 K^+$.

Table I lists the theoretical calculations of the BF and asymmetry parameters of $\Lambda_c^+ \rightarrow \Xi^0 K^+$, as well as the experimental measurements of the BF. Various predictions of the BFs based on the covariant confined quark model (CCQM), the pole model, and current algebra (CA) in the 1990s are all smaller than the experimental results [2]. This is explained as a strong cancellation in the S - and P -wave amplitudes, corresponding to the $L = 0$ and $L = 1$ orbital angular momenta of the Ξ^0 - K^+ system, respectively. Moreover, the decay asymmetry parameter was predicted

to be zero in these models owing to the vanishing S -wave amplitude [7–11]. This long-standing puzzle has recently experienced a renewed interest in the theoretical community [6, 12, 13], especially after the report of new BF measured by BESIII in 2018 [14]. To reproduce the relatively large experimental branching fraction of this decay, Ref. [6] adopted a variant of the CA approach and obtained a larger $\mathcal{B}(\Lambda_c^+ \rightarrow \Xi^0 K^+) \simeq 0.71\%$. This modification introduces a large positive decay asymmetry of 0.90, which is quite close to the calculations based on SU(3) symmetry [12, 13]. However, regarding the significant enhancement of $\alpha_{\Xi^0 K^+}$ from 0 to about 0.9, the authors of Ref. [15] pointed out that the particular construction of the S -wave amplitude in Ref. [6] is not well-justified. So experimental measurement of the asymmetry parameter of the decay $\Lambda_c^+ \rightarrow \Xi^0 K^+$ will be crucial to test these calculations and confirm the vanishing S -wave contribution [15].

In the SM, the amplitude for a spin-1/2 baryon decaying into a spin-1/2 baryon and a spin-0 meson can be written as $\mathcal{M} = i\bar{u}_f(A - B\gamma_5)u_i$, where A and B are constants, u_i and \bar{u}_f are spinors describing the initial and final baryons [8]. For the decay $\Lambda_c^+ \rightarrow \Xi^0 K^+$, the decay asymmetry is defined by $\alpha_{\Xi^0 K^+} = 2\text{Re}(s^*p)/(|s|^2 + |p|^2)$, where $s = A$ and $p = |\vec{p}_{\Xi^0}|B/(E_{\Xi^0} + m_{\Xi^0})$; here E_{Ξ^0} and \vec{p}_{Ξ^0} are the energy and momentum of the Ξ^0 in the Λ_c^+ rest frame [2]. The effect of the S - and P -wave phase shift difference, $\delta_p - \delta_s$, is not well accounted for in the theoretical calculations of decay asymmetries. It can be extracted from experiments combined with the BF cited from the Particle Data Group (PDG) [2] and provides an important experimental parameter for the theoretical prediction of CP violation [16].

In this Letter, we present the first measurement of the decay asymmetry of $\Lambda_c^+ \rightarrow \Xi^0 K^+$ and its decay dynamic parameters ($|A|$, $|B|$, and $\delta_p - \delta_s$). A multidimensional angular analysis of the cascade-decay $e^+e^- \rightarrow \Lambda_c^+ \bar{\Lambda}_c^-$, $\Lambda_c^+ \rightarrow \Xi^0 K^+$, $\Xi^0 \rightarrow \Lambda \pi^0$, and $\Lambda \rightarrow p \pi^-$ is performed using a technique similar to that used to measure the asymmetry parameters of $\Lambda_c^+ \rightarrow p K_S^0$, $\Lambda \pi^+$, $\Sigma^+ \pi^0$, and $\Sigma^0 \pi^+$ [17]. The data samples used in this analysis, with an integrated luminosity of 4.4 fb^{-1} , were collected at center-of-mass (CM) energies of 4.60 (587 pb^{-1}), 4.63 (522 pb^{-1}), 4.64 (552 pb^{-1}), 4.66 (529 pb^{-1}), 4.68 (1667 pb^{-1}), and 4.70 GeV (536 pb^{-1}) with the BESIII detector at the BEPCII collider [18–20]. The values in the parentheses are the corresponding luminosities. Details about BEPCII as well as BESIII and its sub-detectors can be found in Refs. [21–25]. Large data samples taken around the $\Lambda_c^+ \bar{\Lambda}_c^-$ production threshold allow to measure decay asymmetry of low BF decays with the single-tag technique [26]. The low-background environment is more favorable to measure $\alpha_{\Xi^0 K^+}$ accurately. Charge-conjugate modes are always implied unless explicitly stated otherwise.

Simulated event samples produced with a GEANT4-

TABLE I. Theoretical calculations and experimental measurements of the BF, $\alpha_{\Xi^0 K^+}$, $|A|$, $|B|$ and $\delta_p - \delta_s$ of $\Lambda_c^+ \rightarrow \Xi^0 K^+$. G_F is the Fermi constant. The superscript a denotes a model with SU(3) symmetry, while model b includes SU(3) symmetry-breaking effects. The PDG Fit BF also includes a CLEO result on $\mathcal{B}(\Lambda_c^+ \rightarrow \Xi^0 K^+)/\mathcal{B}(\Lambda_c^+ \rightarrow pK^-\pi^+)$ [2].

Theory or experiment	$\mathcal{B}(\Lambda_c^+ \rightarrow \Xi^0 K^+)$ ($\times 10^{-3}$)	$\alpha_{\Xi^0 K^+}$	$ A $ ($\times 10^{-2} G_F \text{ GeV}^2$)	$ B $ ($\times 10^{-2} G_F \text{ GeV}^2$)	$\delta_p - \delta_s$ (rad)
Körner (1992), CCQM [7]	2.6	0
Xu (1992), Pole [8]	1.0	0	0	7.94	...
Żencaykowski (1994), Pole [9]	3.6	0
Ivanov (1998), CCQM [10]	3.1	0
Sharma (1999), CA [11]	1.3	0
Geng (2019), SU(3) [12]	5.7 ± 0.9	$0.94_{-0.11}^{+0.06}$	2.7 ± 0.6	16.1 ± 2.6	...
Zou (2020), CA [6]	7.1	0.90	4.48	12.10	...
Zhong (2022), SU(3) ^a [13]	$3.8_{-0.5}^{+0.4}$	$0.91_{-0.04}^{+0.03}$	3.2 ± 0.2	$8.7_{-0.8}^{+0.6}$...
Zhong (2022), SU(3) ^b [13]	$5.0_{-0.9}^{+0.6}$	0.99 ± 0.01	$3.3_{-0.7}^{+0.5}$	$12.3_{-1.8}^{+1.2}$...
BESIII (2018) [14]	$5.90 \pm 0.86 \pm 0.39$
PDG Fit (2022) [2]	5.5 ± 0.7

based [27] Monte Carlo (MC) package, which provides the geometric description of the BESIII detector and the detector response, are used to determine detection efficiencies and to estimate backgrounds. More details about simulations can be found in Ref. [28]. The phase space MC signal sample is generated uniformly over phase space, which is $e^+e^- \rightarrow \Lambda_c^+ \bar{\Lambda}_c^-$ followed by $\Lambda_c^+ \rightarrow \Xi^0 K^+$, $\Xi^0 \rightarrow \Lambda(\rightarrow p\pi^-)\pi^0(\rightarrow \gamma\gamma)$ and $\bar{\Lambda}_c^-$ decaying inclusively. For the signal MC sample, the signal process is generated by the helicity formalism using the decay asymmetry parameters measured in this work or cited from the PDG [2].

A detailed description of the selection criteria for charged tracks, showers, π^0 , and Λ candidates is provided in Ref. [28]. The only difference is the χ^2 of vertex fit, which constrains the daughter tracks $p\pi^-$ from Λ decays to a common originating vertex, is imposed to be less than 20 in order to better suppress the background. The Ξ^0 candidates are formed by $\Lambda\pi^0$ combinations and the invariant mass $M_{\Lambda\pi^0}$ must be within the mass region (1.30, 1.33) GeV/c^2 . The mass region is selected to be about three times the resolution.

Two kinematic variables, the energy difference $\Delta E \equiv E_{\Lambda_c^+} - E_{\text{beam}}$ and the beam-constrained mass $M_{\text{BC}} \equiv \sqrt{E_{\text{beam}}^2/c^4 - |\vec{p}_{\Lambda_c^+}|^2/c^2}$, are defined to identify $\Lambda_c^+ \rightarrow \Xi^0 K^+$ candidates. Here, $E_{\Lambda_c^+}$ and $\vec{p}_{\Lambda_c^+}$ are the reconstructed energy and momentum of the Λ_c^+ candidates calculated in the e^+e^- rest frame, and E_{beam} is the average energy of the e^+ and e^- beams. All candidates are required to satisfy $|\Delta E| < 0.05 \text{ GeV}$ and $2.25 \text{ GeV}/c^2 < M_{\text{BC}} < E_{\text{beam}}$. If more than one candidate satisfies the above requirements, the one with minimal $|\Delta E|$ is kept. After applying these conditions, the M_{BC} distribution in data collected at 4.60 GeV is

shown in the Fig. 2. In the fit to this data, the correctly and mis-reconstructed signal shapes are modeled with the MC-simulated shape convolved with a Gaussian function representing the resolution difference between data and MC simulation, and the background shape is described by an ARGUS function [29]. Finally, 378 ± 21 signal events are obtained by combining the six energy points.

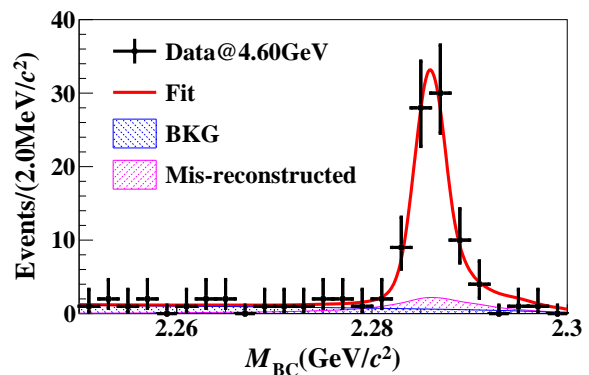


FIG. 2. Distribution of the M_{BC} fitting result at 4.60 GeV, and the corresponding signal yield is 70 ± 8 . Black points with error bars are data; the blue shaded region indicates the combinatorial background events and pink shaded region is the mis-reconstructed signal events.

The decay asymmetry parameters are determined by analyzing the multi-dimensional angular distributions, where the full cascade-decay chain is considered. The joint angular formula is obtained using the helicity basis [30]. Figure 3 illustrates the definitions of the helicity angles for the three-level cascade decay $\Lambda_c^+ \rightarrow \Xi^0 K^+$, $\Xi^0 \rightarrow \Lambda\pi^0$, and $\Lambda \rightarrow p\pi^-$ following the process of $e^+e^- \rightarrow \gamma^* \rightarrow \Lambda_c^+ \bar{\Lambda}_c^-$. In the helicity frame of the $e^+e^- \rightarrow \Lambda_c^+ \bar{\Lambda}_c^-$, θ_0 is the polar angle of the Λ_c^+ with

respect to the e^+e^- beam axis in the e^+e^- CM system. For the $\Lambda_c^+ \rightarrow \Xi^0 K^+$ decay, ϕ_1 is the angle between the $e^+ \Lambda_c^+$ and $\Xi^0 K^+$ planes, and θ_1 is the polar angle of the Ξ^0 with respect to the direction of $\bar{\Lambda}_c^-$ evaluated in Λ_c^+ 's rest frame. For the $\Xi^0 \rightarrow \Lambda \pi^0$ decay, ϕ_2 is the angle between the $\Xi^0 K^+$ and $\Lambda \pi^0$ planes, and θ_2 is the polar angle of the Λ with respect to the direction of K^+ evaluated in Ξ^0 's rest frame. For the helicity angles describing the $\Lambda \rightarrow p \pi^-$ decay, ϕ_3 is the angle between the $\Lambda \pi^0$ and $p \pi^-$ planes, and θ_3 is the polar angle of the proton with respect to the direction of π^0 evaluated in Λ 's rest frame.

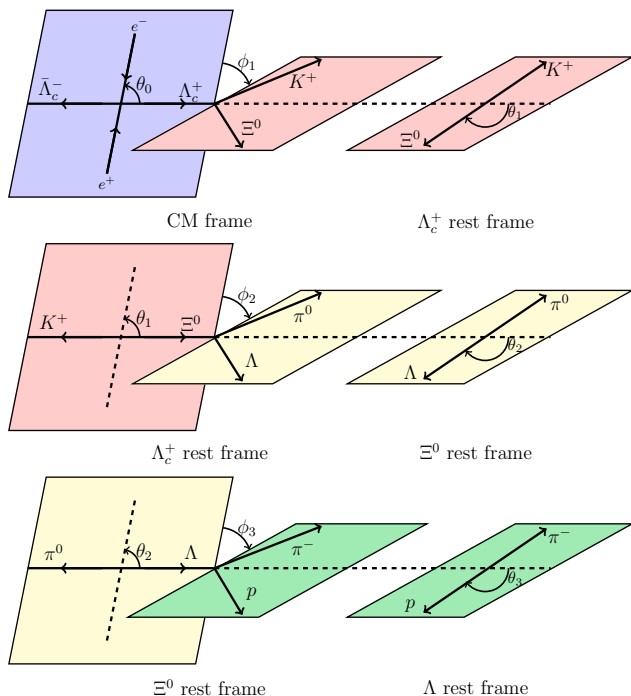


FIG. 3. Definitions of the helicity frames and related angles for $e^+e^- \rightarrow \Lambda_c^+ \bar{\Lambda}_c^-$, $\Lambda_c^+ \rightarrow \Xi^0 K^+$, $\Xi^0 \rightarrow \Lambda \pi^0$, and $\Lambda \rightarrow p \pi^-$.

In Ref. [30], Δ_0 is defined as the phase shift between two individual helicity amplitudes, $\mathcal{H}_{\lambda_1, \lambda_2}$, for the Λ_c^+ production process $\gamma^*(\lambda_0) \rightarrow \Lambda_c^+(\lambda_1) \bar{\Lambda}_c^-(\lambda_2)$ with γ^* 's helicity $\lambda_0 = \pm 1$, and total helicities $|\lambda_1 - \lambda_2| = 0$ and 1, respectively. In the case where one-photon exchange dominates the production process, Δ_0 is also the phase between the electric and magnetic form factors of Λ_c^+ [33, 34], and α_0 is the angular distribution parameter of Λ_c^+ defined by the helicity amplitude $\alpha_0 = (|\mathcal{H}_{1/2, -1/2}|^2 - 2|\mathcal{H}_{1/2, 1/2}|^2) / (|\mathcal{H}_{1/2, -1/2}|^2 + 2|\mathcal{H}_{1/2, 1/2}|^2)$. Similarly, the $\Lambda_c^+ \rightarrow \Xi^0 K^+$ decay is described by two parameters, $\alpha_{\Xi^0 K^+}$ and $\Delta_{\Xi^0 K^+}$, where the latter one is the phase shift between the two helicity amplitudes. The Lee-Yang parameters [30, 35] can be obtained with the relations

$$\begin{aligned} \beta_{\Xi^0 K^+} &= \sqrt{1 - (\alpha_{\Xi^0 K^+})^2} \sin \Delta_{\Xi^0 K^+}, \\ \gamma_{\Xi^0 K^+} &= \sqrt{1 - (\alpha_{\Xi^0 K^+})^2} \cos \Delta_{\Xi^0 K^+}. \end{aligned} \quad (1)$$

In this analysis, the common free parameters ($\alpha_{\Xi^0 K^+}$ and $\Delta_{\Xi^0 K^+}$) describing the angular distributions for the six data sets are determined by a simultaneous unbinned maximum likelihood fit. The likelihood function is constructed from the joint probability density function (PDF) by

$$\mathcal{L}_{\text{total}} = \sum_{\text{energy}} \mathcal{L}_{\text{data}} = \prod_{i=1}^{N_{\text{data}}} f_s(\vec{\xi}_i). \quad (2)$$

Here, $f_s(\vec{\xi}_i)$ is the PDF of the signal process, N_{data} is the number of events in the data and i is the event index. The signal PDF $f_s(\vec{\xi}_i)$ is formulated as

$$f_s(\vec{\xi}_i) = \frac{\epsilon(\vec{\xi}_i) |M(\vec{\xi}_i; \vec{\eta})|^2}{\int \epsilon(\vec{\xi}_i) |M(\vec{\xi}_i; \vec{\eta})|^2 d\vec{\xi}_i}, \quad (3)$$

where $\vec{\xi}_i$ denotes the kinematic angular observables ($\theta_{0,1,2,3}$ and $\phi_{1,2,3}$) and $\vec{\eta}$ denotes the free parameters ($\alpha_{\Xi^0 K^+}$ and $\Delta_{\Xi^0 K^+}$) to be determined. $M(\vec{\xi}_i; \vec{\eta})$ is the total amplitude [30] of all decay chain and $\epsilon(\vec{\xi}_i)$ is the detection efficiency parameterized in terms of the kinematic variables $\vec{\xi}_i$. The background contribution to the joint likelihood is subtracted according to the calculated likelihoods for the combinatorial background based on the inclusive MC simulation and for the misreconstructed signal events based on the signal MC simulation. The integration of the normalization factor is calculated with a large phase space MC sample as

$$\int \epsilon(\vec{\xi}_i) |M(\vec{\xi}_i; \vec{\eta})|^2 d\vec{\xi}_i = \frac{1}{N_{\text{gen}}} \sum_{k_{\text{MC}}}^{N_{\text{MC}}} |M(\vec{\xi}_{k_{\text{MC}}}; \vec{\eta})|^2, \quad (4)$$

where N_{gen} is the total number of the simulated phase space MC events, N_{MC} is the number of the phase space MC events surviving all selection criteria and k_{MC} is the event index.

Using the MINUIT package [36], we minimize the negative logarithmic likelihood with background subtraction over the six data samples. Here, α_0 , Δ_0 , $\alpha_{\Lambda \pi^0}$, $\alpha_{\bar{\Lambda} \pi^0}$, $\Delta_{\Lambda \pi^0}$, and $\Delta_{\bar{\Lambda} \pi^0}$ are fixed to individual values measured by BESIII [37, 38], where the α_0 and Δ_0 can be different at different energy points. $\alpha_{p \pi^-}$ and $\alpha_{\bar{p} \pi^+}$ are fixed to the values from the PDG [2]. In the fit, $\alpha_{\Xi^0 K^+}$ and $\Delta_{\Xi^0 K^+}$ are free parameters, and $\alpha_{\Xi^0 K^+} = -\alpha_{\bar{\Xi}^0 K^-}$ and $\Delta_{\Xi^0 K^+} = -\Delta_{\bar{\Xi}^0 K^-}$ as required under the CP invariance assumption. The projections of the best fit onto several variables are shown in Fig. 4. The data are compared with the MC events weighted by the nominal fitting result. From this fit, we obtain $\alpha_{\Xi^0 K^+} = 0.01 \pm 0.16$ and $\Delta_{\Xi^0 K^+} = 3.84 \pm 0.90$ rad. Hence, the other two Lee-Yang parameters are calculated to be $\beta_{\Xi^0 K^+} = -0.64 \pm 0.69$ and $\gamma_{\Xi^0 K^+} = -0.77 \pm 0.58$, where the uncertainties are statistical only.

The systematic uncertainties arise mainly from the reconstruction of final state particles, which is studied with $J/\psi \rightarrow K_s^0 K^\pm \pi^\mp$ for kaon, $\Lambda_c^+ \rightarrow \Lambda X$ for Λ , $\psi(3686) \rightarrow J/\psi \pi^0 \pi^0$ and $e^+e^- \rightarrow \omega \pi^0$ for π^0 . The systematic uncertainties for ΔE requirement and M_{BC} signal regions are estimated by smearing the phase space MC samples using resolution parameters, and for the background subtraction by taking into account the background shape and size. The uncertainties from the quoted values of α_0 , Δ_0 , $\alpha_{\Lambda\pi^0}$, $\alpha_{\bar{\Lambda}\pi^0}$, $\Delta_{\Lambda\pi^0}$, $\Delta_{\bar{\Lambda}\pi^0}$, $\alpha_{p\pi^-}$ and $\alpha_{\bar{p}\pi^+}$ are estimated by Gaussian sampling considering their uncertainties and refit the angular distribution, and by taking the values in one time uncertainty of Gaussian fit as the uncertainties of this part. A further source of uncertainty is the fit bias, which is the difference before and after the correction from a pull distribution check. Systematic uncertainties from all sources are combined in quadrature to calculate the total systematic uncertainties. All details of systematic uncertainties can be found in Ref. [30].

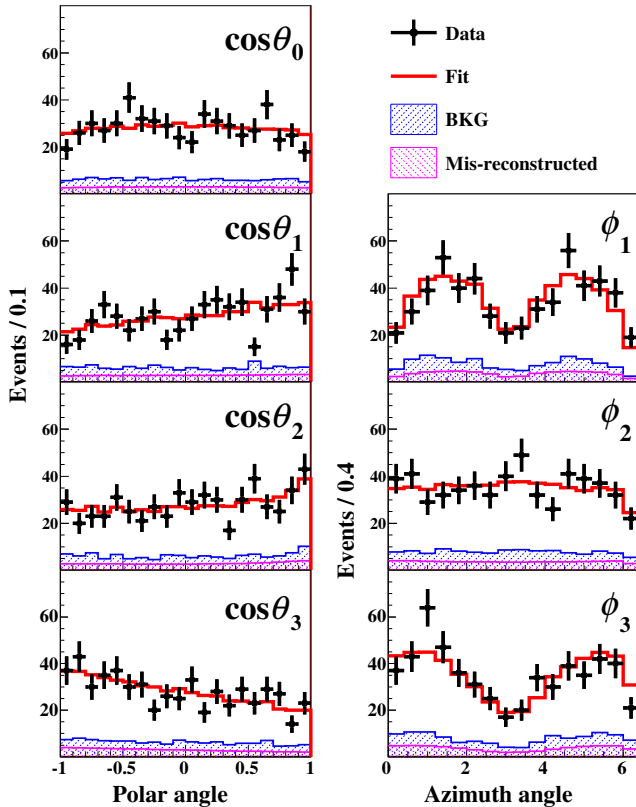


FIG. 4. Projections of the best fit onto various variables. Black points with error bars are data; red solid lines are phase space MC events re-weighted by angular distribution formula, and represent the fitting result; the blue shaded region denotes the combinatorial background events and the pink shaded region is the mis-reconstructed signal events.

One has $\delta_p - \delta_s =$

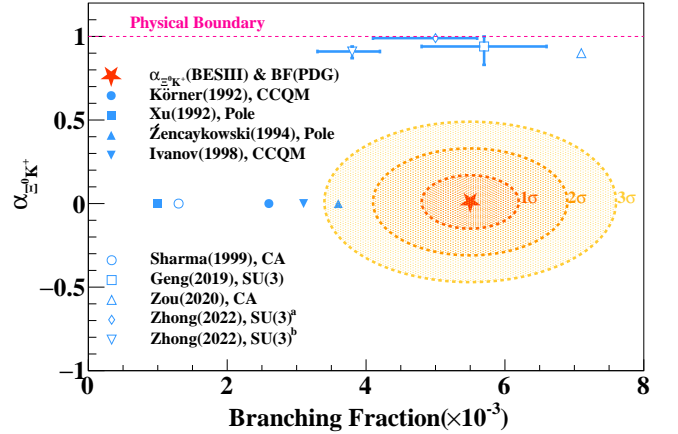


FIG. 5. The comparison between this work and theoretical predictions, where the branching fraction is taken from PDG (2022) [2]. The 1σ , 2σ and 3σ contours correspond to 68.2%, 95.4% and 99.7% confidence level, respectively. The blue symbols are theoretical predictions and the red star is result from this work. The definitions of the superscripts a and b can be found in Table I and the theory acronyms are explained in the text.

$\arctan(\sqrt{1 - \alpha_{\Xi^0 K^+}^2} \sin \Delta_{\Xi^0 K^+} / \alpha_{\Xi^0 K^+})$, and the derivation of $|A|$ and $|B|$ can be found in Ref. [30]. The study has uncovered two distinct physical solutions, with the first one characterized by $|A| = 1.6_{-1.6}^{+1.9}(\text{stat.}) \pm 0.4(\text{syst.})$ and $|B| = 18.3 \pm 2.8(\text{stat.}) \pm 0.7(\text{syst.})$, and the second one by $|A| = 4.3 \pm 0.7(\text{stat.}) \pm 0.2(\text{syst.})$ and $|B| = 6.7_{-6.7}^{+8.3}(\text{stat.}) \pm 1.6(\text{syst.})$.

In summary, by analyzing 4.4 fb^{-1} of e^+e^- annihilation data collected at the CM energies between 4.60 and 4.70 GeV with the BESIII detector, the pure W -boson-exchange decay $\Lambda_c^+ \rightarrow \Xi^0 K^+$ from the $e^+e^- \rightarrow \Lambda_c^+ \bar{\Lambda}_c^-$ production has been studied. The decay asymmetry parameters are measured for the first time as $\alpha_{\Xi^0 K^+} = 0.01 \pm 0.16(\text{stat.}) \pm 0.03(\text{syst.})$ and $\Delta_{\Xi^0 K^+} = 3.84 \pm 0.90(\text{stat.}) \pm 0.17(\text{syst.})$ rad. The other two Lee-Yang parameters are calculated to be $\beta_{\Xi^0 K^+} = -0.64 \pm 0.69(\text{stat.}) \pm 0.13(\text{syst.})$ and $\gamma_{\Xi^0 K^+} = -0.77 \pm 0.58(\text{stat.}) \pm 0.11(\text{syst.})$. The comparison between this work and theoretical predictions is shown in Fig. 5. Our measurement of $\alpha_{\Xi^0 K^+}$ is in good agreement with zero, which is consistent with the theoretical predictions from the 1990s. The decay dynamics parameters $|A|$, $|B|$, and $\delta_p - \delta_s$ are derived. The value of $\delta_p - \delta_s$ has two solutions, which are $\delta_p - \delta_s = -1.55 \pm 0.25(\text{stat.}) \pm 0.05(\text{syst.})$ rad or $1.59 \pm 0.25(\text{stat.}) \pm 0.05(\text{syst.})$ rad. This is of great significance for decay asymmetries, as $\cos(\delta_p - \delta_s)$ measured in this study is close to zero, an effect that had not been anticipated in previous literature. This measurement resolves the long-standing puzzle and deepens our understanding of the strong dynamics in the

charmed baryon sector.

P. R. Li and X. R. Lyu thank Hai-Yang Cheng, Fan-Rong Xu and Fu-Sheng Yu for useful discussions. The BESIII Collaboration thanks the staff of BEPCII and the IHEP computing center for their strong support. This work is supported in part by National Key R&D Program of China under Contracts Nos. 2020YFA0406400, 2020YFA0406300; National Natural Science Foundation of China (NSFC) under Contracts Nos. 11635010, 11735014, 11835012, 11935015, 11935016, 11935018, 11961141012, 12022510, 12025502, 12035009, 12035013, 12061131003, 12192260, 12192261, 12192262, 12192263, 12192264, 12192265, 12221005, 12225509, 12235017; the Chinese Academy of Sciences (CAS) Large-Scale Scientific Facility Program; the CAS Center for Excellence in Particle Physics (CCEPP); Joint Large-Scale Scientific Facility Funds of the NSFC and CAS under Contract No. U1832207; CAS Key Research Program of Frontier Sciences under Contracts Nos. QYZDJ-SSW-SLH003, QYZDJ-SSW-SLH040; 100 Talents Program of CAS; Fundamental Research Funds for the Central Universities, Lanzhou University, University of Chinese Academy of Sciences; The Institute of Nuclear and Particle Physics (INPAC) and Shanghai Key Laboratory for Particle Physics and Cosmology; ERC under Contract No. 758462; European Union's Horizon 2020 research and innovation programme under Marie Skłodowska-Curie grant agreement under Contract No. 894790; German Research Foundation DFG under Contracts Nos. 443159800, 455635585, Collaborative Research Center CRC 1044, FOR5327, GRK 2149; Istituto Nazionale di Fisica Nucleare, Italy; Ministry of Development of Turkey under Contract No. DPT2006K-120470; National Research Foundation of Korea under Contract No. NRF-2022R1A2C1092335; National Science and Technology fund of Mongolia; National Science Research and Innovation Fund (NSRF) via the Program Management Unit for Human Resources & Institutional Development, Research and Innovation of Thailand under Contract No. B16F640076; Polish National Science Centre under Contract No. 2019/35/O/ST2/02907; The Swedish Research Council; U. S. Department of Energy under Contract No. DE-FG02-05ER41374.

-
- [1] G. S. Abrams, M. S. Alam, C. A. Blocker, A. Boyarski, M. Breidenbach, D. L. Burke, W. C. Carithers, W. Chinowsky, M. W. Coles and S. Cooper, *et al. Phys. Rev. Lett.* **44**, 10 (1980).
- [2] R. L. Workman *et al.* (Particle Data Group), *Prog. Theor. Exp. Phys.* **2022**, 083C01 (2022).
- [3] H. Y. Cheng, *Chin. J. Phys.* **78**, 324 (2022).
- [4] H. Y. Cheng, *Sci. Bull.* **67**, 445 (2022).
- [5] F. S. Yu, H. Y. Jiang, R. H. Li, C. D. Lü, W. Wang and Z. X. Zhao, *Chin. Phys. C* **42**, 051001 (2018).
- [6] J. Zou, F. Xu, G. Meng and H. Y. Cheng, *Phys. Rev. D* **101**, 014011 (2020).
- [7] J. G. Körner and M. Krämer, *Z. Phys. C* **55**, 659 (1992).
- [8] Q. P. Xu and A. N. Kamal, *Phys. Rev. D* **46**, 270 (1992).
- [9] P. Zenczykowski, *Phys. Rev. D* **50**, 5787 (1994).
- [10] M. A. Ivanov, J. G. Körner, V. E. Lyubovitskij and A. G. Rusetsky, *Phys. Rev. D* **57**, 5632 (1998).
- [11] K. K. Sharma and R. C. Verma, *Eur. Phys. J. C* **7**, 217 (1999).
- [12] C. Q. Geng, C. W. Liu and T. H. Tsai, *Phys. Lett. B* **794**, 19 (2019).
- [13] H. Zhong, F. Xu, Q. Wen and Y. Gu, *JHEP* **02**, 235 (2023).
- [14] M. Ablikim *et al.* (BESIII Collaboration), *Phys. Lett. B* **783**, 200 (2018).
- [15] S. Groote and J. G. Körner, *Eur. Phys. J. C* **82**, 297 (2022).
- [16] J. P. Wang and F. S. Yu, [arXiv:2208.01589 \[hep-ph\]](https://arxiv.org/abs/2208.01589)
- [17] M. Ablikim *et al.* (BESIII Collaboration), *Phys. Rev. D* **100**, 072004 (2019).
- [18] M. Ablikim *et al.* (BESIII Collaboration), *Chin. Phys. C* **46**, 113002 (2022).
- [19] M. Ablikim *et al.* (BESIII Collaboration), *Chin. Phys. C* **46**, 113003 (2022).
- [20] B. C. Ke, J. Koponen, H. B. Li and Y. Zheng, *Ann. Rev. Nucl. Part. Sci.* **73**, 285-314 (2023).
- [21] M. Ablikim *et al.* (BESIII Collaboration), *Nucl. Instrum. Meth. A* **614**, 345 (2010).
- [22] C. H. Yu *et al.*, *Proceedings of IPAC2016, Busan, Korea, 2016*.
- [23] M. Ablikim *et al.* (BESIII Collaboration), *Chin. Phys. C* **44**, 040001 (2020).
- [24] J. W. Zhang, L. H. Wu, S. S. Sun, J. H. Zou, C. X. Liu, Z. Y. Deng, Q. M. Ma, S. P. Wen, G. F. Cao and B. L. Zhang, *et al. Rad. Det. Tech. Meth.* **6**, 289-293 (2022).
- [25] X. Li *et al.*, *Rad. Det. Tech. Meth.* **1**, 13 (2017); Y. X. Guo *et al.*, *Rad. Det. Tech. Meth.* **1**, 15 (2017); P. Cao *et al.*, *Nucl. Instrum. Meth. A* **953**, 163053 (2020).
- [26] H. B. Li and X. R. Lyu, *Natl. Sci. Rev.* **8**, nwab181 (2021).
- [27] S. Agostinelli *et al.* (GEANT4 Collaboration), *Nucl. Instrum. Meth. A* **506**, 250 (2003).
- [28] M. Ablikim *et al.* (BESIII Collaboration), *Chin. Phys. C* **47**, 023001 (2023).
- [29] H. Albrecht *et al.* (ARGUS Collaboration), *Phys. Lett. B* **241**, 278-282 (1990).
- [30] See Supplemental Material at <https://journals.aps.org/prl/supplemental/10.1103/PhysRevLett.132.031801> for the Lee-Yang parameters, joint angular distribution formula, details of the systematic uncertainties, and the relation with weak decay amplitude, which includes Refs. [31, 32].
- [31] E. P. Wigner, *Pure Appl. Phys.* **5**, 142 (1959).
- [32] M. Ablikim *et al.* (BESIII Collaboration), *Phys. Rev. Lett.* **121**, 062003 (2018).
- [33] G. Fäldt, *Phys. Rev. D* **97**, 053002 (2018).
- [34] M. Ablikim *et al.* (BESIII Collaboration), *Phys. Rev. Lett.* **120**, 132001 (2018).
- [35] T. D. Lee and C. N. Yang, *Phys. Rev.* **108**, 1645 (1957).
- [36] F. James and M. Roos, *Comput. Phys. Commun.* **10**, 343 (1975).
- [37] M. Ablikim *et al.* (BESIII Collaboration), *Phys. Rev. Lett.* **131**, 191901 (2023).

- [38] M. Ablikim *et al.* (BESIII Collaboration), [Phys. Rev. D **108**, L031106 \(2023\)](#).